Influence of oxygen vacancies on electronic and magnetic properties of Ni (5%)-doped SnO_2 nanorods

K. Srinivas and P. Venugopal Reddy*
*Department of Physics, Osmania University, Hyderabad, 500007, INDIA
*paduruvenugopalreddy@gmail.com

ABSTRACT

With a view to study the influence of nanometric size and surface effects on the structural, electronic and magnetic properties of Ni (5%) doped SnO_2 diluted magnetic semiconductor (DMS) nanorods, prepared by PEG-6000 assisted wet chemical route, a systematic investigation has been carried out. The structural and surface morphological properties investigated by several characterization techniques clearly indicate that the samples of present investigation are having nanorod like morphology with single phase, polycrystalline tetragonal rutile structure without any detectable impurity phases. The XPS core level Ni 2p spectra indicate the oxidation state of Ni as +2. Further, a detailed analysis of XPS, optical absorbance and PL results were carried out to understand the local electronic structure, lattice disorder and oxygen vacancies. The Magnetization measurements were carried out to understand the magnetic behaviour with varying nanometric size of the samples. These studies revealed that, all the samples are found to exhibit clear room temperature ferromagnetism. Interestingly, the magnetic behaviour of the samples is found to depend critically on the random distribution or diffusive nature of Ni ions, oxygen vacancies with varying the annealing temperature, aspect ratio and the surface condition of nanorods. Further, the ESR and Magnetic Force Microscopic (MFM) studies clearly ruled out the presence of magnetic clusters and their magnetic contribution. Finally, the origin of RT ferromagnetism has been discussed using dopant – defect hybridization induced bound magnetic polaron theory.

Keywords: magnetic semiconductors, SnO_2 nanorods, electronic structure, ferromagnetism

1 INTRODUCTION

Oxide based DMSs (ODMSs) such as Zn (TM) O and (Sn, Ti, Hf) $(TM)O_2$ [TM: Co, Ni, Fe, Mn, etc.,] have attracted the attention of the scientific community as they exhibit ferromagnetism with Curie temperatures (T_C) at or above room temperatures. Their functionality is linked to the wide band gaps and can be doped heavily with *n*-type carriers and are ideal for short wavelength applications. The need for environmental friendly ODMS has prompted an intense search for materials exhibiting large Zeeman splitting of the electronic bands and giant Faraday rotation around room temperature. Although ferromagnetism was reported above room temperature in a number of oxide based dilute magnetic semiconductors, studies on Ni doped SnO_2 is of particular interest due to their higher effective mass, native oxygen vacancies, high carrier density, high transparency along with the possibility of tunable magnetic, optical, surface and interface properties.

Due to peculiar structural characteristics and size effects, nanostructured oxide based DMSs often exhibit novel physical and chemical properties, different from those of the micro crystalline ones. Especially, one dimensional (1D) nanostructured based materials have two quantum-controlled directions, while still leaving one unconfined direction for electrical conduction and their surface to volume ratio is much greater than the coarse materials so that the surface properties become paramount. Therefore, the work on 1D nanostructured oxide based DMSs has become a new frontier of research to explore their potential applications in nanoscale spintronics , magneto – optical, high density data storage, non–volatile memory devices, nanomagnetic fluids and magnetic sensors[1-3]. Earlier, the synthesis of Ni doped SnO_2 nanorods and their structural and magnetic properties were published by the authors of present investigation [4]. However, the present work is the extension of the earlier work and is aimed at studing the influence of nanometric size and oxygen vancancies in 1D nanostructured Ni-doped SnO_2 DMSs. The details such results are presented here.

2 EXPERIMENTAL

Ni – doped (5%) SnO_2 nanorods were prepared by PEG (Poly ethylene glycol – 6000) assisted wet chemical method. In this method, high purity starting precursors of $SnCl_4.5H_2O$ (0.06431617 moles) and $NiCl_2.6H_2O$ (0.003385 moles) were converted into tartarates using tartaric acid (TA) taken in the ratio, metal ions to TA as 1:2. Later, 10ml poly ethylene glycol (PEG) taken from 100 gl^{-1} of PEG (PEG average molecular weight, 6000 $gmol^{-1}$), was added to the resultant solution with continuous stirring. , Aqueous ammonia was added slowly by maintaining the reaction temperature at about 50 ^oC, until pH is reached to a value between 6 and 7. The resulting gel was then dried and washed with double distilled water using centrifuge. Finally, the precursor was calcined at 250 ^oC for 6 hrs and annealed at different temperatures between 350 – 650 ^oC for 3 hrs in air. More details are given in an earlier pubication [4].

The XRD patterns were recorded using a Phillips (X 'pert) diffractometer with Cu– K_α radiation (λ = 1.5406 A°) in the range of 20 – 80°. Atomic Force Microscopy

studies were undertaken with CP-II, Veeco Instruments by using phosphorus (n) doped Si probes. Transmission electron microscopy (TEM) studies were undertaken using JEOL JEM-200CX at 160 kV.The Raman spectral studies were carried out at room temperature by using a WiTec GmbH confocal micro Raman equipped with a CCD detector. The light source was a Nd:YAG laser of 532 nm wavelength. X – ray photoelectron spectroscopic (XPS) measurements were performed on a KRATOS AXIS165 X–ray photoelectron spectrometer using excitation energy of 1253.6 eV (Mg Kα). Optical absorbance measurements were undertaken at room temperature using UV-visible spectrophotometer (Model: Evolution 300, Thermo electron corporation) in the wavelength range 200 to 600 nm. The Photo Luminescence studies were carried out to understand the behaviour of oxygen vacancies using fluorolog spectro fluorimeter (Jyobin Vyon) with a 450 W Xenon lamp source. Magnetization studies were undertaken both as a function of field (upto 15 kOe) and temperature over a temperature range 80 – 300 K at a constant applied field 500 Oe using a Vibrating Sample Magnetometer (Model: DMSADE-1660 MRS). Electron Spin Resonance spectra were also recorded at room temperature on a JOEL PE-3X X-band spectrometer equipped with 9153.593 MHz field modulation unit. All ESR measurements were carried out using DPPH (g = 2.00455) as a standard. Finally, the Magnetic Force Microscopy (MFM) studies were undertaken in MFM mode of an Atomic Force microscope (AFM model CP-II Veeco Instruments) using commercial CoCr coated SiN probe (model: MESP).

3 RESULTS AND DISCUSSION

The Rietveld refined XRD patterns of Ni doped (5%) SnO_2 samples annealed at different temperatures are shown in Fig. 1. The diffraction peaks are in good agreement with the JCPDS data of SnO_2 (JCPDS 41-1445). The lattice parameter were evaluated using the Rietveld whole X-ray profile fitting by MAUD 2.14 software and are given in Table I. A careful quantitative phase analysis of the samples revealed that doped Ni ions are successfully incorporated in the host lattice without forming any detectable impurity phases. Further, both the cell parameters 'a' and 'c' are found to increase gradually with increasing annealing temperature and nanometric size of the samples. It can be seen from Table- 1 that with increasing annealing temperature, 'c/a' (lattice distortion) values are found to increase systematically .This behaviour may be attributed to increase in the internal residual tensile stress/strain originated during the growth of one dimensional nanograins. In fact, lattice distortion in these nanorods might also depends on the surface effects. With decreasing grain size, the surface to volume ratio goes up, enhancing the surfacial tension which is responsible for the lattice dilatation in the nanorods of Ni-doped (5%) SnO_2 .

The surface topography images recorded using AFM are shown in Fig 2. These images are found to appear as an array of aggregated nanorod shape like morphology in all the samples. From various line profile measurements of individual nanorods on different samples, the average

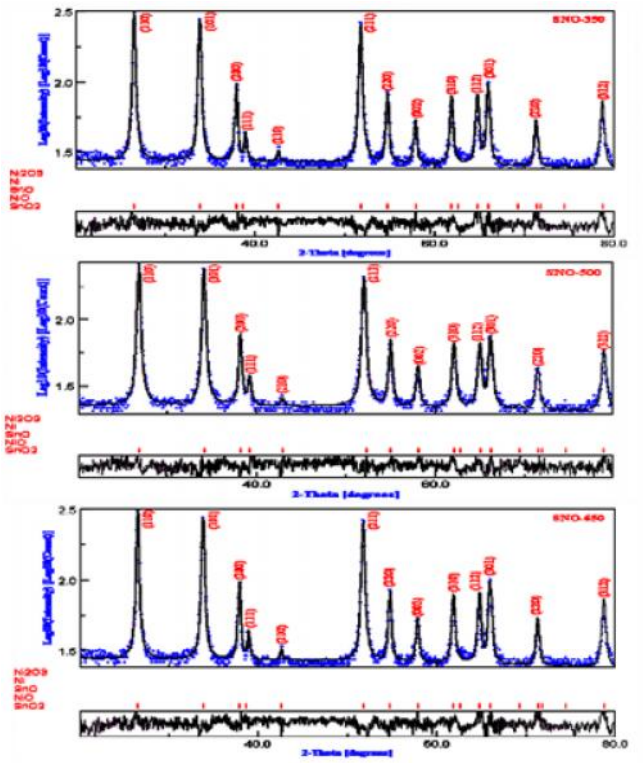

Figure 1: Rietveld Refined XRD patterns of Ni – (5%) doped SnO_2, annealed at different temperatures.

aspect ratio is found to increase from ~2.85 to 10.21 (Table 1) with increasing annealing temperature. In addition to AFM topography studies, TEM studies were also performed on dispersed powder samples and Surface morphology and corresponding SAED patterns are ahown in Fig 3. These images confirm the formation of nanorods like morphology and their aspect ratios are given in Table 1. In the samples of present investigation, the average lengths of the nanorods are found to increase from ~25 to 230 nm with increasing annealing temperature, while their average widths increase from ~10 to 30 nm.

Table 1: Rietveld refined XRD data and aspect ratio of Ni doped SnO2 annealed at different temperatures.

Sample code		**SNO-350**	**SNO-500**	**SNO-650**
Annealing Temperature (˚C)		350	500	650
Rietveld refined XRD data	**<a> (Å)**	4.735	4.739	4.744
	<c> (Å)	3.184	3.189	3.194
	(c/a)	0.67254	0.67277	0.67327
	R_w (%)	6.79	7.97	7.41
	R_{exp} (%)	4.76	5.46	5.68
	R_b (%)	7.20	7.03	6.49
Aspect Ratio	**From AFM**	2.85	6.78	10.21
	From TEM	3.02	6.95	10.2

The Gaussian fitted Ni 2p XPS core level spectra are shown in Fig. 4(A) and and O1s XPS peaks are shown in Fig. 4(B). The positions of Ni $2p_{3/2}$ and Ni $2p_{1/2}$ are found to be

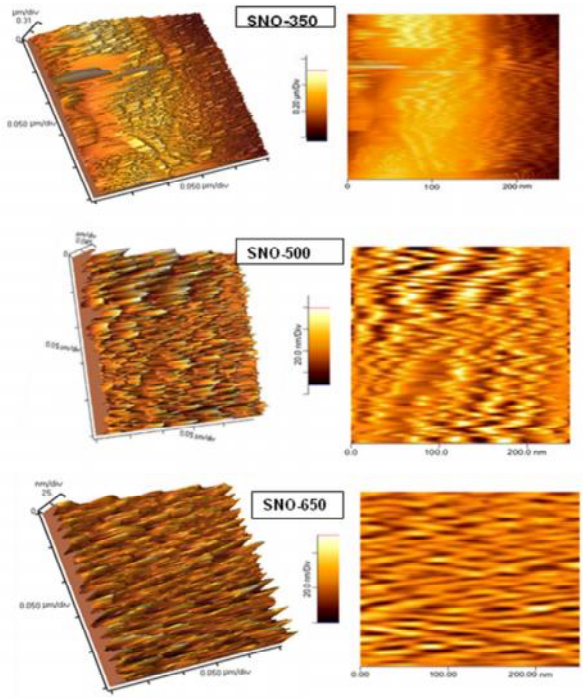

Figure 2: AFM 2D and corresponding 3D topography images of Ni – (5%) doped SnO_2, annealed at different temperatures.

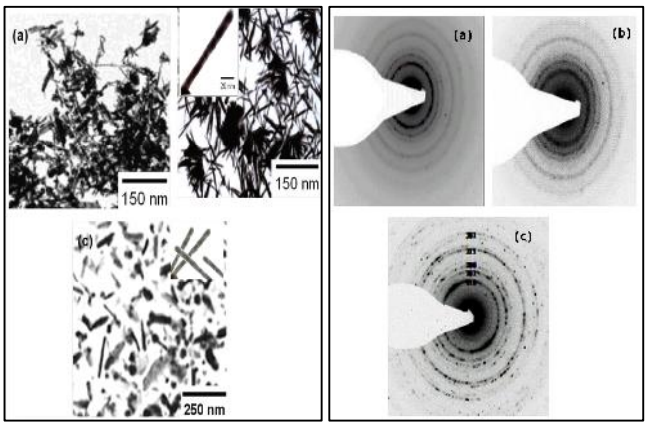

Figure. 3 (A) TEM surface topography images and (B) SAED patterns of a) SNO-350, b) SNO-500 and c)SNO-650 samples respectively.

in the range ~ 855.35 – 855.12 eV and ~ 872.695 – 872.978 eV respectively. The characteristics of divalent nickel Ni(II) were confirmed based on the peak positions of Ni $2p_{3/2}$ (in the range of ~853.3 – 854.4 eV) and the shake–up satellite peak (at ~860.1 eV). From these results, it has been concluded that Ni $2p_{3/2}$ positions are different from those of Ni (~852.3 eV), NiO (~853.4 eV) and Ni_2O_3 (~856.7 eV).

As the energy difference between Ni $2p_{3/2}$ and Ni $2p_{1/2}$ peaks ranges from 17.308 – 17.850 eV, the absence of NiO (18.4 eV) may be ruled out. Due to local charge imbalance created by random distribution of Ni^{2+} ions, the local or surface defects such as oxygen vacancies might have been formed. Therefore, the variation in binding energy values of core level Ni 2p is dependent on the number of oxygen vacancies. The O1s spectrum shows three – component oxygen peaks. From these results, the peak (1) around ~ 531.5 – 532.7 eV may be attributed to O_2^{2-}, O^- and OH^- ions in the oxygen deficient regions[36], where as the peak (2) around ~ 530 – 531 eV may be due to the related lattice oxygen, O – Sn – O bonds, and O^{2-} ions. Finally, the peak (3) in the range ~528 – 529 eV might be attributed O_2^- ions adsorbed on the surface of SnO_2:Ni nanorods.

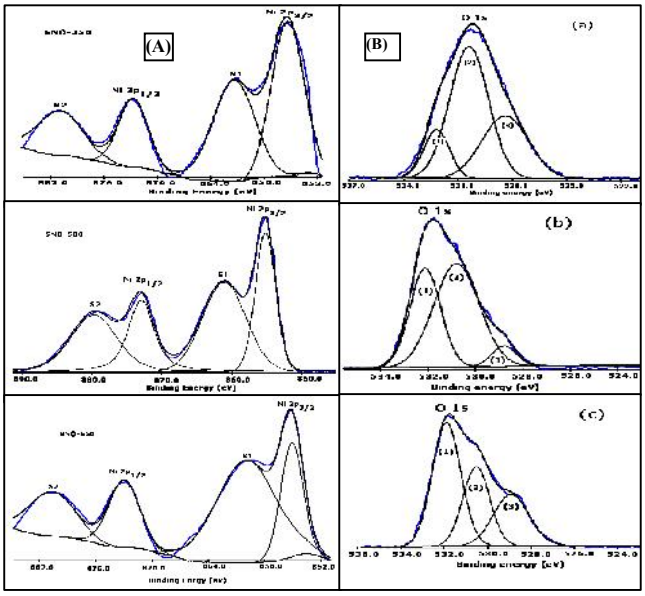

Figure 4: XPS Ni2p and O1s core level spectra of Ni – (5%) doped SnO_2 nanorods.

From optical absorption spectra band gap values are calculated and are found to increase with increasing annealing temperature. In other word, with decreasing the aspect ratio, the band gap values are found to decrease gradually indicating a clear red shift and may be attributed to the strain induced disorder or surface defects. The oxygen vacancies, and local disorder combinedly lead to changes in the local electronic structure of the materials. In the present investigation, the emission spectra were recorded at excitation wavelengths (λ_{ex}) of 365 and are shown in Fig. 5(a). All the samples are found to exhibit a strong UV emission at ~396 nm (3.13 eV) and a weak broad blue emission peak at ~ 471 nm (2.63 eV). The peak around ~396 nm (3.13 eV) is assigned to the direct recombination of conduction electrons in Sn 4p band and a hole in O 2p valence band. The intensity of the emission peaks are found to decrease with increasing annealing temperature and the behaviour may be due to decreasing oxygen vacancies. The Raman spectra of Ni (5%) doped SnO_2 nanorods annealed at different temperature is shown in Fig. 5(b). Three fundamental Raman modes of Ni doped (5%) SnO_2 nano – rods viz., E_g at ~ 472 – 474 cm^{-1}, A_{1g} at ~ 619 – 632 cm^{-1}, and B_{2g} at ~768 – 774 cm^{-1} are similar to those of tetragonal rutile undoped SnO_2 nanorods[ ], confirming the absence of impurity phases and the observation is consistent with the XRD results. ESR spectra of all the samples (Figure 5(c)) are found to exhibit a broad resonance peak, denoted by the signal 'A' and the Lande's *g* factor (g_{eff}) of the broad signal '*A'* is found to be higher [3.16 - 3.33] when compared with the free radical g value.

It is interesting to note that the position of signal 'A' is located relatively at a lower field along with broad nature, indicating a clear ferromagnetic signature of the materials.

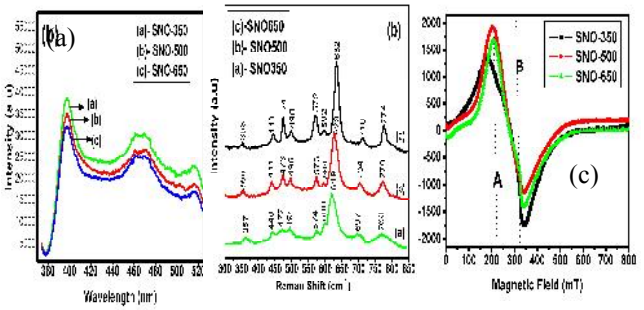

Figure.5 (a)Photo luminiscence, (b) Raman spectra and (c) ESR spectra of a) SNO-350, b) SNO-500 and c) SNO-650 samples respectively.

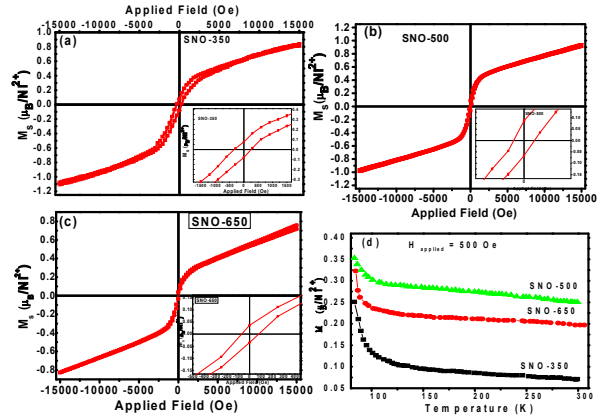

Figure 6. M-H curves of a) SNO-350, b) SNO-500, c) SNO- 650 samples and d) M-T plot of all the samples.

M– H hysteresis curves of all the samples are shown in Fig. 6 (a, b, c) . The inset images shows their corresponding remanence and coercivities. It is interesting to note that all the samples of the present investigation are found to exhibit clear room temperature ferromagnetism. The maximum magnetic moment obtained in the present investigation is 0.925 μ_B/Ni^{2+} for the samples of SNO-500 nanorods. The magnetic moment is found to decrease with decreasing oxygen vacancy concentration. Figure 6(d) shows the variation of magnetization with temperature M (T) in a field of 500 Oe. With increasing temperature the magnetization value are found to decrease due to thermal vibrations become strong enough to overcome the Zeeman interactions and initiate randomization of the magnetic moments. The M-T curve shows a nonzero magnetization even at room temperature, indicating that the Curie temperatures of the samples of present investigations might be above 300 K. Figure 7. shows MFM images of all the samples. The magnetic domain pattern over the surface of the samples seems to a strip like behaviour. The observed bright and dark contrasts in the MFM images clearly indicate the formation of magnetic domains. The room temperature ferromagnetism might have originated due to the interactions among the dopant and defect induced percolated bound magnetic polarons in $Sn_{1-x}Ni_xO_2$ single phase nano rods. In fact, the effective ferromagnetic exchange interactions might have also linked with the unpaired electron spins originated from oxygen vacancies at the surface of nanorods. In fact, the effective interactions between BMPs depend on the dopant induced defects, the complex behaviour of exchange media and the distribution of Ni ions. However, still extensive studies are required to understand the local ferromagnetic behaviour and to exploit features of nanostructured spintronic devices with varying nanometric size and annealing temperature of $Sn_{1-x}Ni_xO_{2-x}$ nanorods.

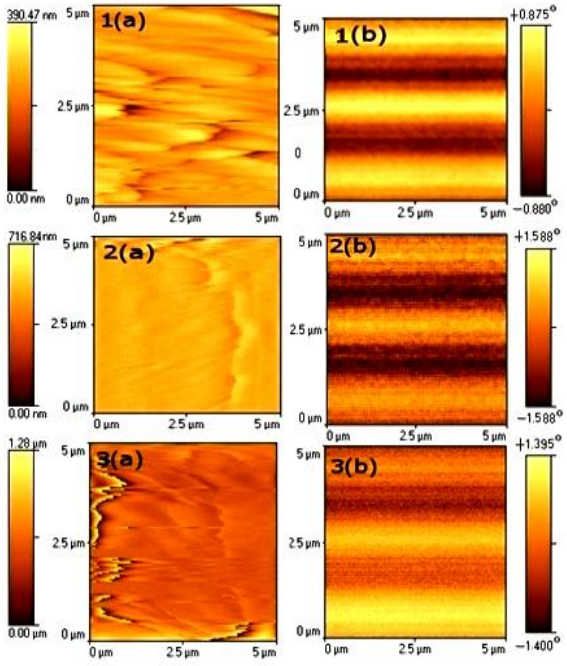

Figure 7. Magnetic Force microscopy topography images (without lift) and their corresponding magnetic phase images (at lift height 80 nm) of a) SNO-350, b) SNO-500 and c) SNO- 650 samples respectively.

4 CONCLUSIONS

In summery, single phase and high quality Ni doped (5%) SnO_2 DMS nanorods are found to exhibit clear room temperature ferromagnetism without any impurity phases. As the nanometric size, oxygen vacancies and local electronic structure of the samples are interlinked, it has been concluded that the magnetic behaviour clearly depends on the dopant distribution or the inter – diffusion behaviou and the surface chemistry of nanograins.

REFERENCES

[1] Q. Xu, L. Hartmann, S. Zhou, A. Mcklich, K. Potzger, M. Helm, G. Biehne, H. Hochmuth, M. Lorenz, M.Grundmann and H. Schmidt, Phys. Rev. Lett. 2008, 101, 076601.

[2] S. Han, D. Zhang and C. Zhou, Appl. Phys. Lett. , 2006, 88, 133109.

[3] A.Punnoose, K. M. Reddy, J. Hays, A. Thurber and M. H. Engelhard, Appl. Phys. Lett., 2006, 89, 112509.

[4] K. Srinivas,S. Manjunath Rao and P. Venugopal Reddy, Nanoscale, 2011, 3, 642-653.